An engineered construct combining complement regulatory and surface recognition domains represents a minimal-size functional factor H[1]

Mario Hebecker[*], María Alba-Domínguez[†], Lubka T. Roumenina[‡,§,¶], Stefanie Reuter[*], Satu Hyvärinen[‖], Marie-Agnès Dragon-Durey[‡,§,¶,#], T. Sakari Jokiranta[‖], Pilar Sánchez-Corral[†], and Mihály Józsi[*,**,2]

[*]Junior Research Group Cellular Immunobiology, Leibniz Institute for Natural Product Research and Infection Biology – Hans Knöll Institute, Jena, Germany; [†]Research Unit, Hospital Universitario La Paz – IdiPAZ, and CIBER de Enfermedades Raras, Madrid, Spain; [‡] Cordeliers Research Center, INSERM UMRS 872, 75 006 Paris, France; [§] Université Pierre et Marie Curie (UPMC-Paris-6), 75 006 Paris, France; [¶] Université Paris Descartes, Sorbonne Paris Cité 75 006 Paris, France; [‖]Department of Bacteriology and Immunology and Immunobiology Research Program, Haartman Institute, University of Helsinki, FI-00014 Helsinki, Finland; [#]Hopital Europeen Georges-Pompidou, Service d'Immunologie Biologique, APHP, 75908 Paris Cedex 15, France; [**]MTA-ELTE "Lendület" Complement Research Group, Department of Immunology, Eötvös Loránd University, Budapest, Hungary

Corresponding author: Mihály Józsi, MTA-ELTE "Lendület" Complement Research Group, Department of Immunology, Eötvös Loránd University, Pázmány Péter sétány 1/c, H-1117 Budapest, Hungary; Phone: +36 1 3812175; Fax: +36 1 3812176; E-mail: mihaly.jozsi@gmx.net.

Running title: Mini-factor H as a complement inhibitor

Abstract

Complement is an essential humoral component of innate immunity; however, its inappropriate activation leads to pathology. Polymorphisms, mutations and autoantibodies affecting factor H (FH), a major regulator of the alternative complement pathway, are associated with various diseases, including age-related macular degeneration, atypical hemolytic uremic syndrome and C3 glomerulopathies. Restoring FH function could be a treatment option for such pathologies. Here we report on an engineered FH construct that directly combines the two major functional regions of FH, the N-terminal complement regulatory domains and the C-terminal surface recognition domains. This minimal-size FH (mini-FH) binds C3b and has complement regulatory functions similar to those of the full-length protein. In addition, we demonstrate that mini-FH binds to the FH-ligands C-reactive protein, pentraxin 3 and malondialdehyde epitopes. Mini-FH was functionally active when bound to the extracellular matrix and endothelial cells *in vitro* and inhibited C3 deposition on the cells. Furthermore, mini-FH efficiently inhibited complement-mediated lysis of host-like cells caused by a disease-associated FH mutation or by anti-FH autoantibodies. Therefore, mini-FH could be potentially used as a complement inhibitor targeting host surfaces, and to replace compromised FH in diseases associated with FH dysfunction.

Introduction

The complement system is a major humoral component of innate immunity, participating in the protection against infections, removal of immune complexes, waste disposal, and regulation of the adaptive immune response (1). It is activated via three major pathways, namely the classical, the lectin and the alternative pathways. Complement activation is targeted and limited both in time and space. The activation of this plasma enzyme system is controlled by several fluid-phase and cell-bound complement regulators that intervene at various points of the activation cascade. The alternative pathway is spontaneously and constantly activated in plasma at a low rate. In addition, all three pathways lead to activation of C3 via C3 convertase enzymes, and the generated C3b molecules can form additional alternative pathway C3 convertases and thus amplify complement activation. Therefore, proper regulation of the alternative pathway is essential (2). Misdirected or systemic, overwhelming activation leads to complement-associated diseases, such as age-related macular degeneration (AMD),[3] atypical hemolytic uremic syndrome (aHUS) and C3 glomerulopathies, including C3 glomerulonephritis and dense deposit disease (DDD) (1-5). A number of complement inhibitors are being developed with the hope of applying them in the treatment of such diseases (6).

Factor H (FH) is the major regulator of the alternative pathway in plasma and it also plays an important complement inhibitory role when attached to host cell surfaces and basement membranes (7,8). FH is a 150-kDa glycoprotein with a plasma concentration ~250 µg/ml (9). It regulates the alternative pathway C3 convertase (C3bBb) through three mechanisms. First, it competes with factor B for C3b binding, thus inhibiting convertase formation. Second, it enhances the decay of existing convertases by displacing the C3b-

bound Bb fragment. Third, it acts as a cofactor for the protease factor I in the cleavage and irreversible inactivation of C3b. By these mechanisms, FH down-regulates the alternative complement pathway (7). Mutations, polymorphisms and autoantibodies affecting FH, which are associated with AMD, aHUS, DDD and other C3 glomerulopathies, influence the ability of FH to interact with C3b and/or with host cells or extracellular ligands, thus causing alterations in the activity of this important complement regulator (10-12).

FH is composed of 20 complement control protein domains (CCPs; also known as short consensus repeat domains, SCRs). The N-terminal domains 1-4 of FH are necessary and sufficient for the cofactor and decay accelerating activities of the protein (13, 14). The crystal structure of FH domains 1-4 with C3b and that of factor I revealed the molecular basis for the cofactor and decay accelerating activities of FH, indicating that FH facilitates C3b cleavage by providing a binding platform for factor I and stabilizing the domain structure of C3b, while promoting destabilization of the C3 convertase through competition and electrostatic repulsion (15, 16). In host cell recognition by FH, the C-terminal domains 19-20 play a critical role, targeting the complement regulatory activity of FH to the surfaces of host cells and tissues (17, 18). Recent reports on the structure of the FH domains 19-20 in complex with C3d provided structural insights into this host protection mechanism (19, 20). Collectively, these data suggest a folded-back structure of FH when bound to C3b on a surface, with CCP4 and CCP19 coming into proximity (15, 19-21).

FH-based therapeutics could be of advantage over certain current treatments, such as plasma infusion or Eculizumab, which inhibits complement at a later step (5). Purified full-length FH already demonstrated its efficacy in controlling the C3 convertase in a mouse model of FH deficiency (22) and in *in vitro* C3 deposition and cell protection assays in the presence of aHUS-associated anti-FH autoantibodies or mutations in FH or C3 (23-25). Domains 19-20, which naturally evolved to dock FH on host cells, could be exploited in drug design to direct the regulatory activity of FH, or other complement inhibitor, to host surfaces (26). Therefore, we speculated that a minimal-size functional FH (mini-FH) could be created by directly fusing the complement regulatory domains and the host cell recognition domains of FH. This notion gathered further support from structural data published recently (19, 20). We generated such a construct that is limited to the two major functional regions, i.e. domains 1-4 and 19-20, and assessed the functional activity of this recombinant protein as a potential therapeutic complement inhibitor alternative to purified or recombinant full-length FH.

Materials and Methods

The study was performed in accordance with the Declaration of Helsinki and was approved by the Research Ethics Committees of the Medical Faculty of the Friedrich Schiller University (control number 2269-04/08), of the University Hospital 'La Paz' and Comité de Protection des Personnes Ile de France V (IDRCB2008-A00144-51). Informed consent was obtained from the probands or their parents before obtaining plasma samples for the experiments.

Proteins, sera and antibodies

Mini-FH was generated by gene synthesis (GenScript, Piscataway, NJ). Nucleotides coding for CCPs 1-4 and CCPs 19-20 from the FH cDNA sequence (accession number Y00716) were codon-optimized, synthesized, cloned into the pBSV-8His Baculovirus expression vector, expressed in *Spodoptera frugiperda* (Sf9) cells, and purified by nickel-affinity chromatography as described (27). Recombinant FH-related protein 1 (CFHR1), the FH fragments consisting of CCPs 1-4 (FH1-4) and CCPs 15-20 (FH15-20) were generated and produced as described (28).

FH was purified from normal human serum (29) or obtained from Merck Chemicals Ltd. (Schwalbach, Germany) or from Complement Technologies (Tyler, Texas, US). C2-depleted serum, C3, C3b, C3d, factor I, factor B, factor D, properdin, goat anti-human factor H antibody and goat anti-human factor B antibody were purchased from Merck, and FH-depleted serum, C3b and C3d were from Complement Technologies. Horseradish peroxidase (HRP)-conjugated goat anti-human C3 was from MP Biomedicals (Solon, OH). Rabbit anti-human C3d antibody was obtained from Dako (Hamburg, Germany). HRP-conjugated swine anti-rabbit immunoglobulins and rabbit anti-goat immunoglobulins were from Dako. The mAb C18 was from Alexis Biochemicals (Lörrach, Germany). The mAb OX24 was purchased from Santa Cruz Biotechnology (Heidelberg, Germany). Anti-C3c antibody was from Quidel (Teco Medicals, Paris, France).

Sequence analyses
Nucleotide and protein sequences were analyzed using the Bioinformatics Resource Portal (ExPASy) of the Swiss Institute of Bioinformatics (www.expasy.org) with the Translate, the Compute pI/Mw and the ProtParam tools.

Microtiter plate binding assays
To analyze C3b and C3d binding, 100 nM mini-FH or FH, diluted in Dulbecco's phosphate-buffered saline (DPBS; Lonza, Wuppertal, Germany), were immobilized in microtiter plates. Nonspecific binding sites were blocked with DPBS containing 3% bovine serum albumin (Sigma-Aldrich, Taufkirchen, Germany). Serial dilutions of C3b and C3d in DPBS were added for 1 h at 22°C, and binding was detected using HRP-conjugated anti-C3 (for C3b) or anti-C3d antibody followed by the respective secondary antibody. TMB PLUS substrate (Kem-En-Tec Diagnostics, Taastrup, Denmark) was used to visualize antibody binding and the absorbance was read at 450 nm.

Binding of mini-FH and FH to wells coated with MaxGel (diluted 1:30), gelatin (25 µg/ml), PTX3 (10 µg/ml; ~30 nM) and CRP (10 µg/ml; ~87 nM) was performed as for C3b and C3d but using DPBS containing Ca^{2+} and Mg^{2+} (Lonza).

Real time binding assay
The interaction of FH and mini-FH with C3b and C3d was analyzed in real time using a ProteOn XPR36 surface plasmon resonance (SPR) equipment (BioRad). C3b and C3d were immobilized by a standard amine coupling technology to GLC biosensor chip. Different concentrations of FH or mini-FH were injected simultaneously through the 6 channels of the microfluidic system at 30 µl/min flow rate and allowed to interact with each of the three immobilized proteins for 300 s. The dissociation was followed also for 300 s. The running buffer was 10 mM Hepes, 140 mM NaCl and 0.005% Tween-20, pH 7.2. The surface was regenerated with an 18 s pulse of 25 mM NaOH. The experiment was repeated three times on two different chips. Bivalent analyte binding model was used to calculate the apparent kinetic parameters since it was the closest to the real situation, where FH has two binding sites for C3b in domains 1-4 and 19-20. The 1:1 Langmuir model was used for C3d binding, since only domains 19-20 participate in the interaction. Binding curves were double referenced by subtracting the signal from the interspots and the signal from a buffer injection as recommended by the manufacturer.

MAA-BSA binding assay for FH, mini-FH and FH1-4
Malondialdehyde sodium salt (MDA•Na) was synthesized from 1,1,3,3-tetramethoxypropane (Sigma-Aldrich) as previously described (30) and then used in modification of BSA (fatty acid free; Sigma-Aldrich) with a protocol modified after Thiele *et al.*, and Ishii *et al.* (30, 31) Briefly, BSA (2 mg/ml) was incubated overnight in 0.1 M phosphate (pH 7.2) with MDA•Na (50 mM) and acetaldehyde (20 mM) in rotation at 37°C until vividly yellow. The modification product was named MAA-BSA as both malondialdehyde and acetaldehyde were used in modification (malondialdehyde-acetaldehyde-adduct of BSA). Unreacted aldehydes were removed by changing the MAA-BSA into PBS with a concentrator (Amicon Ultra-15 Ultracel 30k). The modification of the lysines of BSA by MDA was analyzed by increase in mobility under native PAGE (fluorescence detected by Fluoroskan, ex/em 355/460 nm).

Microtiter plate wells were coated with 15 µg/ml MAA-BSA at 4°C for 17 h. The wells were blocked with 0.5% BSA/PBS for 1 h, then washed with 0.05% Tween-20 in PBS, and incubated with dilution series of purified FH (32), recombinant mini-FH or FH1-4 prepared in 0.1% BSA/PBS for 1 h at 22°C. The wells were washed with 0.05% Tween-20/PBS, and then incubated with mAb 90X (33) (4 µg/ml in 0.1% BSA/PBS) for 1 h at room temperature. After thorough washing, HRP-conjugated anti-mouse-Ab (Jackson ImmunoResearch; 0.7 µg/ml in 0.1% BSA/PBS) was added for 1 h at 22°C. After thorough washing, ortho-phenylenediamine (OPD, Dako) was added according to the manufacturer's instructions and the bound HRP-conjugated antibody was quantitated by reading absorbance at 492 nm. In data analysis, the A492 nm reading of BSA (wells that were blocked only) for each FH, mini-FH or FH1-4 dilution was subtracted from the respective A492 nm value for MAA-BSA.

C3 convertase decay assay
Solid-phase alternative pathway C3 convertase was assembled on immobilized C3b in microtiter plate wells as described previously (34). Increasing concentrations of mini-FH or FH were added for 30 min at 37°C, and the remaining intact convertase was determined using a goat anti-factor B antiserum. TMB PLUS substrate was used to visualize antibody binding and the absorbance was read at 450 nm.

Cofactor assays

Cofactor activity of mini-FH and FH was measured in fluid-phase assays by incubating C3b (220 nM) and factor I (440 nM) with 10 nM FH or mini-FH for 1 h at 37°C in a final volume of 20 µl. The reactions were stopped by adding reducing SDS-sample buffer. Samples were loaded onto 11% SDS-PAGE gels, separated by electrophoresis and subjected to Western blot. C3 fragments were revealed using HRP-conjugated goat anti-human C3 and an enhanced chemiluminescence detection kit (Applichem, Darmstadt, Germany).

To assay cofactor activity on surfaces, 50 µl of 1 µM mini-FH or FH were added to wells coated with MaxGel (diluted 1:30 in DPBS containing Ca^{2+} and Mg^{2+}), gelatin (25 µg/ml), PTX3 (30 nM) or CRP (87 nM), and incubated for 1 h at 22°C After washing, 140 nM C3b and 220 nM factor I, diluted in DPBS, were added in 50 µl to the wells, and incubated for 1 h at 37°C. Reducing SDS-sample buffer was added to the supernatants, which were then run on 11% SDS-PAGE and subjected to Western blotting. C3 degradation products were identified as described above.

The cofactor activity of mini-FH on HUVEC (American Type Culture Collection, Rockville, MD, USA) was measured by incubating 3×10^5 cells with 2 µM mini-FH or FH in a final volume of 50 µl in DPBS at 37°C for 1 h. After washing, cells were incubated with 220 nM C3b and 440 nM factor I in 50 µl for 45 min at 37°C. Supernatants were analyzed for C3b cleavage as described above.

Mini-FH binding to cells

Binding of mini-FH to HUVEC was measured by incubating the cells with 2 µM FH or mini-FH as described for the cofactor assay. Binding was measured by flow cytometry as described previously (18), using goat anti-FH antibody and FITC-conjugated rabbit anti-goat Ig (Dako) for the detection. Dead cells were excluded from the analysis based on propidium iodide staining. 10,000 cells were measured in a BD LSRII flow cytometer and data were analyzed by the FACSDiva (BD Biosciences, Heidelberg, Germany) and FlowJo (Tree Star, Ashland, OR, USA) softwares. Binding of mini-FH and FH were also visualized from HUVEC lysed with DPBS containing 1% Triton X-100 and Complete Protease Inhibitor Cocktail (Roche, Mannheim, Germany) for 45 min on ice. The cell extracts were separated on 11% SDS-PAGE under non-reducing conditions, the proteins transferred to nitrocellulose membranes, and the blots were developed using goat anti-FH antibody followed by HRP-conjugated secondary antibody.

Binding of mini-FH to SRBC (BioTrend Chemikalien, Cologne, Germany) was detected by Western blotting. SRBC were incubated with 15% C2-depleted plasma with 2 µM mini-FH at 37°C for 30 min, and the binding was visualized from cell lysates as described above.

C3 deposition on endothelial cells

The C3 deposition on HUVEC in presence of FH-depleted serum was performed as described previously (24). Briefly, primary HUVEC at passage 3 were activated with 10 ng/ml TNFα, 10^3 U/ml IFNγ and 10 ng/ml IL-1 overnight, washed and incubated with 30% FH-depleted serum diluted in M199 medium containing 5 mM Ca^{2+} and Mg^{2+} and different doses of FH or mini-FH. After 30 min/37°C/CO_2, the cells were washed with PBS, detached with PBS-BSA-EDTA and labelled with 10 µg/ml mouse anti-C3c, followed by anti-mouse-PE secondary antibody. Cells were gated based on morphology, data were collected and analyzed by a FACSCalibur instrument (BD Biosciences) using FCS Express Software (De Novo software). The experiment was performed three times using HUVEC from two different healthy donors.

Hemolysis assays

To assess the role of mini-FH in host cell protection from complement-mediated damage, SRBC were used in various hemolysis assays measuring alternative pathway-mediated lysis, as described previously (35, 36). To determine whether mini-FH causes anomalous lysis by competing with FH, mini-FH, FH15-20 and CFHR1 were added at 2 µM final concentration to SRBC and 15% C2-depleted human plasma in a final volume of 100 µl. The reactions were incubated at 37°C for 30 min, the red cells sedimented by centrifugation, and the released hemoglobin was measured in the supernatants at 414 nm.

SRBC lysis induced by the mAb C18, which binds to CCP20 of FH and inhibits FH binding to cells (18), was performed by adding 2 µg of the mAb C18 to 15% C2-depleted human plasma, used to allow complement activation via the alternative pathway only, in a final volume of 100 µl. SRBC lysis induced by the mAb OX24 (1.6 µg), which binds to CCP5 and inhibits the complement regulatory domains of FH, was measured in 10% normal human serum as described (35). SRBC lysis caused by plasma from an aHUS patient with the W1183L mutation in heterozygosis (23) or from an aHUS patient with anti-FH autoantibodies were analyzed

as described (35). FH and mini-FH were added and their inhibitory effect on SRBC lysis was determined as previously described (35).

Statistical analysis
Statistical analysis was performed using GraphPad Prism version 4.00 for Windows (GraphPad Software, San Diego California USA). A p value < 0.05 was considered statistically significant.

Results

Generation of mini-FH
We hypothesized that a mini-FH that would keep the C3b- and host surface binding properties of FH could be generated (**Fig. 1A and 1B**). To construct mini-FH, the original nucleotide sequence of exons 2-5 and 22-23 of the *CFH* gene, coding for domains 1-4 and 19-20, respectively, were codon-optimized (**Supplementary Fig. 1)**, synthesized and cloned into the Baculovirus expression vector pBSV-8His (27). This construct has no artificial linker between the domains 4 and 19, only the native six amino acids between the fourth cysteine in CCP4 and the first cysteine in CCP19. The translated protein has a theoretical pI of 6.32 and a molecular mass of 42,233 Da (44,891 Da with the His-tag). We hypothesized that such a mini-FH would be able to regulate surface C3b as does full-length FH (**Fig. 1B**). The protein was expressed in insect cells and purified by nickel-affinity chromatography; the average protein yield was ~8.2 mg/L cell supernatant (**Fig. 1C**).

Interaction of mini-FH with C3b and C3d and analysis of its functional activity in regulation of C3b
First, we tested the ability of the mini-FH construct to bind to C3b, the main FH ligand, which binds to both domains 1-4 and 19-20 (37, 38). Equimolar amounts of FH and mini-FH were immobilized in microtiter plate wells and the binding of increasing concentrations of C3b was measured. C3b bound to FH and mini-FH in a similar dose-dependent manner (**Fig. 2A**). These data further support FH domains 1-4 and 19-20 as the main binding sites for fluid-phase C3b, although additional sites have been reported (37, 38). We also tested the binding of C3d, which is bound by the domains 19-20 (37). C3d bound more strongly to mini-FH than to FH (about fourfold) (**Fig. 2B**), which may indicate a better availability of the C-terminal C3d binding site in the compact mini-FH in comparison with FH.

To assess binding of mini-FH to surface-bound C3 fragments and to avoid the need of a detection antibody, a label-free SPR detection system was used with C3b and C3d immobilized on biosensor chip (**Fig. 3**). The binding of mini-FH to C3b showed different interaction mode compared to FH. Mini-FH showed overall threefold stronger binding, when the resonance unit (RU) at the same time point and the same molar concentration was compared to that of FH (**Fig. 3A and Table I**). Nevertheless, mini-FH had approximately 2.5-fold slower association rate but formed 1.3-fold more stable complexes compared to FH, resulting in twofold weaker affinity. Mini-FH bound much stronger to C3d compared to FH. At identical molar concentration (25 nM), the residual amount of mini-FH in the C3d-coated chip was more than 80-fold higher compared to FH. The association rate of mini-FH was 8.5-fold slower than that of FH but this was compensated for by 22-fold slower dissociation, resulting in a 2.6-fold higher affinity (**Fig. 3B and Table I**).

We then tested the capacity of mini-FH to accelerate the decay of the alternative pathway C3 convertase (C3bBb), which was assembled on immobilized C3b. The spontaneous, the FH-mediated and the mini-FH-mediated decay of the convertase was measured. Mini-FH displayed strong decay accelerating activity similar to that of FH (**Fig. 4A**). We also analyzed the activity of mini-FH as a cofactor for the factor I-mediated cleavage of C3b. Mini-FH displayed cofactor activity similar to that of FH (**Fig. 4B**). These data indicate that in the functional assays *in vitro* mini-FH is at least as efficient as the native, full-length protein.

Mini-FH binds to pentraxins
Other physiological FH ligands are the pentraxins C-reactive protein (CRP) and PTX3, which may direct the complement inhibitory activity of FH to sites of inflammation (39, 40). Both CRP and PTX3 bind to CCP20 of FH (40-43). Mini-FH bound to CRP and PTX3 in a dose-dependent manner (**Fig. 5A**). Its binding to PTX3 was similar to that of FH, whereas mini-FH showed weaker binding to CRP compared with FH. This might be explained by the presence of an additional CRP binding site in CCP7 of FH (39), which is missing in mini-FH. Accordingly, CRP-bound FH displayed stronger cofactor activity than mini-FH, whereas the cofactor activities of FH and mini-FH when bound to PTX3 were comparable (**Fig. 5B**).

Mini-FH binds to malondialdehyde (MDA) epitopes

Recently, MDA epitopes formed during oxidative damage have also been shown to bind domains 19-20 of FH (44). We used immobilized BSA modified with MDA and acetaldehyde (MAA-BSA) as a model of MDA-epitope containing surfaces. For the detection of the bound FH and mini-FH proteins, we used the mAb 90X, which recognizes CCP1 (33). We found that mini-FH bound to MAA-BSA, but its binding was clearly weaker than that of FH, as expected, since an additional MDA epitope binding site, within FH domain 7, is missing in mini-FH (**Fig. 6A**). Mini-FH showed dose-dependent binding, while FH1-4, used as a negative control, did not show binding to MAA-BSA (**Fig. 6B**).

Mini-FH is functionally active when bound to extracellular matrix or endothelial cells

Self/nonself discrimination by FH is important to protect host cells and noncellular surfaces, such as the kidney glomerular basement membrane, from complement attack. Therefore, the binding of mini-FH to extracellular matrix (ECM) and its complement regulatory activity on such surface were analyzed and compared with those of FH. We used the human basement membrane extract MaxGel for these studies (43). Mini-FH showed similar dose-dependent binding to MaxGel as FH (**Fig. 7A**). FH and mini-FH did not show specific binding to gelatin, used as negative control. ECM-bound mini-FH displayed cofactor activity similar to that of FH (**Fig. 7B**).

Mini-FH bound also to human umbilical vein endothelial cells, used as a model of host endothelial cells (18), although according to the flow cytometry analysis the binding efficiency seemed lower than that of FH, because of the fewer epitopes in mini-FH recognized by the detection antibody (**Fig. 8A, B**). However, the cell-bound mini-FH displayed cofactor activity comparable to that of FH (**Fig. 8C**). Mini-FH was more efficient in the protection of endothelial cells from complement attack compared to FH, when added to FH-depleted serum. Mini-FH was 2.4-fold more efficient in reaching 50% inhibition of C3 deposition (approximately 0.22 μM FH *versus* 0.09 μM mini-FH) (**Fig. 8D**).

Mini-FH reverses the anomalous host cell lysis caused by FH mutations and autoantibodies

The relevance of the FH C-terminus in the protection of host surfaces by FH is indicated by disease-associated mutations and autoantibodies affecting this part of the molecule (10, 11). *In vitro*, C-terminal fragments of FH, such as FH19-20 and FH15-20, compete with full-length FH for binding to host cells while failing to provide complement regulation due to the lack of domains 1-4. Therefore, these fragments cause impaired host cell protection by occupying cellular FH binding sites. When added to human plasma, FH19-20 or FH15-20 cause anomalous lysis of SRBC (17, 35), which are used as an *in vitro* model of host-like cells.

We used hemolytic assays to assess the protective activity of mini-FH in a host cellular model using C2-depleted serum. Mini-FH bound to SRBC (**Fig. 9A**), but in contrast to FH15-20, it did not cause cell lysis up to the tested 2 μM concentration (~90 μg/ml), as expected due to the presence of the complement regulatory domains in this construct (**Fig. 9B**). As a control, we also used FH-related protein 1 (CFHR1), which does not effectively bind to the cells and does not therefore inhibit cellular binding of FH (35) (**Fig. 9A, B**).

The mAb C18 binds to CCP20 of FH and inhibits FH binding to host cells (18, 45), resulting in improper protection of the cells from complement-mediated lysis (35, 36). Because the aHUS-associated anti-FH autoantibodies share a binding site on FH with this mAb (25, 46), it can be used to mimic the action of autoantibodies (35). We tested the capacity of mini-FH and FH to inhibit the SRBC lysis induced by mAb C18. Both proteins showed a dose-dependent lysis inhibitory effect, but mini-FH was more effective (~fourfold) than FH (**Fig. 9C**).

Similarly, anti-FH autoantibody-positive plasma of aHUS patients causes hemolysis of SRBC because the autoantibodies block FH binding to the cells (25, 36). Addition of purified FH reverses this anomalous lysis very efficiently (**Fig. 9D**) (25, 35). Likewise, mini-FH inhibited SRBC lysis caused by anti-FH autoantibodies in patient-derived plasma (**Fig. 9D**). In addition, we tested whether mini-FH can prevent hemolysis caused by a mutation (W1183L) in the C-terminal surface recognition domain of FH (23). Again, mini-FH showed a dose-dependent inhibitory effect, stronger than that of FH (**Fig. 9E**). Furthermore, the anomalous SRBC lysis caused by the mAb OX24, which inhibits the N-terminal complement regulatory domains, could be reversed by the addition of mini-FH (**Fig. 9F**).

Recently, an overall neutralization of FH by autoantibodies in the acute phase of autoimmune aHUS has been described (47). Plasma samples containing autoantibodies against multiple FH epitopes were collected at the very onset from three patients diagnosed with the autoimmune form of aHUS. The autoantibodies in these samples bound to both the N- and C-termini of FH, and in the case of patient 2, also to the central part of FH. In the hemolysis assays performed as described (47), mini-FH strongly inhibited the

SRBC lysis induced by the autoantibodies (**Fig. 10**). In this assay, mini-FH was also more effective in inhibiting the hemolysis than FH.

Discussion

FH is a major complement regulator whose deficiency or altered function due to mutations or autoantibodies is associated with several diseases. In some of these diseases, such as aHUS, the therapy includes plasma infusion or plasma exchange, which provide functional FH (48). Purified FH could be used to replace the dysfunctional protein in the acute phase of such diseases.

FH is a large molecule with multiple cysteine bridges and therefore its recombinant production is not easy and cheap, although production of recombinant full-length FH has recently been reported (49, 50). Here, we describe mini-FH, a compact form of FH limited to the two main functional regions, as a potent complement inhibitor. Such a construct has several advantages over human plasma-derived, purified FH. It can be expressed in large quantities with standardized quality and concentration. There are no batch-to-batch differences in protein sequence as it would be in plasma purified FH because of common and rare polymorphisms and occasional mutations. When using recombinant material, there is also no risk of transmitting infectious agents such as prions and viruses. Moreover, availability of human material does not limit production. A disadvantage could be the lack of natural posttranslational modifications of FH, about which the current knowledge is unsatisfactory. However, post-translational modifications such as glycosylation of FH have not been shown to be functionally important, and in the case of mini-FH glycosylation appears not to be a problem because domains 1-4 and 19-20 present in the mini-FH are not glycosylated in the native FH (51). Regarding potential immunogenicity, the lack of artificial linker sequences minimizes the risk of autoimmune reaction; however, this needs to be further tested *in vivo*.

In this study we have characterized mini-FH (i) for binding to the FH ligands C3b, C3d, CRP, PTX3 and MDA-epitopes; (ii) for decay acceleration of solid-phase C3 convertase and for cofactor activity in the fluid phase and when bound to various ligands; and (iii) for binding and functional activity on host cellular surfaces (ECM, endothelial cells and SRBC).

Mini-FH bound to the tested FH ligands, including the main ligand C3b (**Fig. 2, 3**), as well as C3d, pentraxins and MAA-BSA (**Fig. 5, 6**). Mini-FH is able to regulate C3b by retaining the complement regulatory functions of FH (**Fig. 4.**). Interestingly, mini-FH bound stronger to C3d than FH. This may be explained by the better availability of the C3d binding site in the compact mini-FH molecule compared to FH. The differences in the binding mode of FH and mini-FH to C3b on the sensor chip could reflect the physiological situation on the cell surface, where FH can bind to two adjacent C3b molecules (one with CCPs 1-4 and another with CCPs 19-20) due to the presence of a long stretch of 14 domains (CCPs 5-18) between the two binding sites. Such binding was suggested to be more physiologically relevant compared to the one when FH wraps around the same C3b molecule (51). In contrast, mini-FH can bind only to one C3b molecule and this can assure better anchoring (by domains 19-20) of the regulatory domains CCPs 1-4 to the same C3b molecule. This and/or the stronger residual binding of mini-FH to C3b compared to FH could be a reason why mini-FH proved to be a more efficient inhibitor of C3 deposition on HUVEC and of the complement-mediated SRBC lysis in comparison with full-length FH (**Fig. 8-10**). Even though mini-FH has only a short linker sequence between domains 4 and 19, it worked rather well in the ligand binding and functional assays. However, further optimization of the linker may improve the structural flexibility and thus the activity of the protein.

The pentraxins PTX3 and CRP, which activate complement on one hand, have been shown, on the other hand, to bind the efficient down-regulator of complement activation FH, and suggested to target FH to the sites of inflammation (39, 40). Both pentraxins were shown to interact with FH via domains 7 and 20 (39-43). In addition, disease-associated FH variants have been shown to have impaired binding to CRP or PTX3 (41, 43, 52, 53). For PTX3, the main binding site in FH was localized to CCP20 (43) and mini-FH, although lacking the CCP7 domain, showed comparable PTX3 binding and complement regulatory activity when bound to PTX3 as the full-length FH (**Fig. 5**). The AMD-associated FH polymorphic variant 402H binds less efficiently to CRP than the 402Y variant, suggesting an impaired function in the clearance of cellular debris and regulation of inflammation (52-54). Mini-FH could compensate for the impaired binding of FH to surface-bound CRP caused by pathogenic mutations in FH domain 20 (41). Since our results showed weaker binding and activity of mini-FH on CRP, compared with that of FH, mini-FH might not fully compensate for the impaired FH function caused by mutations/polymorphisms in domain 7 (**Fig. 5**).

Recently, MDA epitopes were shown to bind FH through two sites, one in domain 7 and another in domains 19-20 (44). The importance of MDA-binding of FH *in vivo* is not clear yet, but it has been suggested to be involved in the pathogenesis of AMD causing blindness since the AMD-associated 402H variant of FH

showed reduced binding to MDA, resulting in reduced local protection from oxidative stress (44). As mini-FH contains only one MDA-epitope binding site compared to the two sites in full FH, it was expected to show weaker binding than FH, as observed. Thus, mini-FH likely confers reduced protection from complement activation to surfaces containing MDA-epitopes compared with full-length FH.

FH also interacts with the extracellular matrix and protects from excessive complement activation on this surface (43). Mini-FH showed comparable cofactor activity to FH when bound to the model ECM (**Fig. 7**). This activity is likely relevant in renal diseases where FH binding to the glomerular basement membrane is primarily mediated by CCPs 19-20 and impaired FH binding was suggested to play a role in disease pathogenesis (43, 55).

An important function of FH is its participation in the protection of host cells from complement attack. Our *in vitro* assays demonstrate that recombinant mini-FH rescues host cells from complement-mediated damage caused by FH mutations, FH deficiency or autoantibodies associated with aHUS. Mini-FH also compensates for FH dysfunction in the N-terminal complement regulatory domains, demonstrated by assays using the mAb OX24, which mimics autoantibodies associated with DDD (56-58). Autoantibodies against the N-terminal domains of FH have recently also been described in the acute phase of aHUS (47), and mini-FH very efficiently protected the SRBC from hemolysis caused by such antibodies (**Fig. 10**). Therefore, mini-FH could be potentially applied as a complement inhibitor in diseases in which dysregulation of the complement alternative pathway is particularly implicated, such as aHUS and C3 glomerulopathies (59, 60). The applicability may not be limited to FH-related disorders, since addition of purified FH was able to control the increased complement activation on endothelial cell surface in the presence of sera of aHUS patients with C3 mutation (24). Nevertheless, attention should be paid since certain mutations in factor B or C3 are resistant to regulation by FH, and C3 nephritic factors may also render the C3 convertase resistant to regulation (61-65). Mini-FH could likely also be used to protect erythrocytes from complement-mediated damage in paroxysmal nocturnal hemoglobinuria (PNH) patients (66). FH plays a role in the protection of PNH erythrocytes, which are characterized by strongly reduced numbers of the membrane-anchored complement regulatory proteins CD55 and CD59 due to a defect of glycosyl-phosphatidylinositol anchor (67). A recent report showed that targeting CCPs 1-5 of FH to sites of complement activation at the surface of PNH erythrocytes by using a chimeric molecule confers protection of these erythrocytes from C3 fragment deposition and lysis (68).

Due to the C-terminal domains designed by nature to direct FH to sites of ongoing complement activation, mini-FH is expected to down-regulate complement activation under various pathological conditions. Our data demonstrate that mini-FH retains the complement regulatory activity of FH and it is likely more active on a molar basis. The therapeutic use of mini-FH requires further studies, but the results shown suggest its potential use in the treatment of kidney diseases, such as aHUS and C3 glomerulopathies.

Acknowledgments

We thank Eliška Svobodová for help with flow cytometry and Barbara Uzonyi for helpful suggestions. We also thank the Department of Infection Biology (Hans Knöll Insitute, Jena) for access to their flow cytometer and blot developer. We thank Professor Reija Jokela and Heli Flink (Laboratory of Organic Chemistry, Aalto University, Finland) for their help with the synthesis of malondialdehyde sodium salt.

References

1. Ricklin, D., G. Hajishengallis, K. Yang, and J. D. Lambris. 2010. Complement: a key system for immune surveillance and homeostasis. *Nat. Immunol.* 11: 785-797.
2. Zipfel, P. F., S. Heinen, M. Józsi, and C. Skerka. 2006. Complement and diseases: defective alternative pathway control results in kidney and eye diseases. *Mol. Immunol.* 43: 97-106.
3. Roumenina, L. T., C. Loirat, M-A. Dragon-Durey, L. Halbwachs-Mecarelli, C. Sautes-Fridman, and V. Fremeaux-Bacchi. 2011. Alternative complement pathway assessment in patients with atypical HUS. *J. Immunol. Methods.* 365: 8-26.
4. Fakhouri, F., V. Frémeaux-Bacchi, L. H. Noël, H. T. Cook, and M. C. Pickering. 2010. C3 glomerulopathy: a new classification. *Nat. Rev. Nephrol.* 6: 494-499.
5. Rodríguez de Cordoba, S., A. Tortajada, C. L. Harris, and B. P. Morgan. 2012. Complement dysregulation and disease: from genes and proteins to diagnostics and drugs. *Immunobiology* 217: 1034-1046.
6. Ricklin, D. and J. D. Lambris. 2007. Complement-targeted therapeutics. *Nat. Biotechnol.* 25: 1265-1275.

7. Ferreira, V. P., M. K. Pangburn, and C. Cortés. 2010. Complement control protein factor H: the good, the bad, and the inadequate. *Mol. Immunol.* 47: 2187-2197.
8. Dinasarapu, A. R., A. Chandrasekhar, M. Józsi, and S. Subramaniam. 2012. Complement Factor H. *UCSD Molecule Pages,* doi:10.6072/H0.MP.A004256.01
9. Hakobyan, S., C. L. Harris, A. Tortajada, E. Goicochea de Jorge, A. García-Layana, P. Fernández-Robredo, S. Rodríguez de Córdoba, and B. P. Morgan. 2008. Measurement of factor H variants in plasma using variant-specific monoclonal antibodies: application to assessing risk of age-related macular degeneration. *Invest. Ophthalmol. Vis. Sci.* 49: 1983-1990.
10. Józsi, M. and P. F. Zipfel. 2008. Factor H family proteins and human diseases. *Trends Immunol.* 29: 380-387.
11. Boon, C. J., N. C. van de Kar, B. J. Klevering, J. E. Keunen, F. P. Cremers, C. C. Klaver, C. B. Hoyng, M. R. Daha, and A. I. den Hollander. 2009. The spectrum of phenotypes caused by variants in the CFH gene. *Mol. Immunol.* 46: 1573-1594.
12. Servais, A., L. H. Noël, L. T. Roumenina, M. Le Quintrec, S. Ngo, M-A. Dragon-Durey, M. A. Macher, J. Zuber, A. Karras, F. Provot, B. Moulin, J. P. Grünfeld, P. Niaudet, P. Lesavre, and V. Frémeaux-Bacchi. 2012. Acquired and genetic complement abnormalities play a critical role in dense deposit disease and other C3 glomerulopathies. *Kidney Int.* 82: 454-464.
13. Gordon, D. L., R. M. Kaufman, T. K. Blackmore, J. Kwong, and D. M. Lublin. 1995. Identification of complement regulatory domains in human factor H. *J. Immunol.* 155: 348-356.
14. Kühn, S. and P. F. Zipfel. 1996. Mapping of the domains required for decay acceleration activity of the human factor H-like protein 1 and factor H. *Eur. J. Immunol.* 26: 2383-2387.
15. Wu, J., Y. Q. Wu, D. Ricklin, B. J. Janssen, J. D. Lambris, and P. Gros. 2009. Structure of complement fragment C3b-factor H and implications for host protection by complement regulators. *Nat. Immunol.* 10: 728-733.
16. Roversi, P., S. Johnson, J. J. Caesar, F. McLean, K. J. Leath, S. A. Tsiftsoglou, B. P. Morgan, C. L. Harris, R. B. Sim, and S. M. Lea. 2011. Structural basis for complement factor I control and its disease-associated sequence polymorphisms. *Proc. Natl. Acad. Sci. U S A.* 108: 12839-12844.
17. Ferreira, V. P., A. P. Herbert, H. G. Hocking, P. N. Barlow, and M. K. Pangburn. 2006. Critical role of the C-terminal domains of factor H in regulating complement activation at cell surfaces. *J. Immunol.* 177: 6308-6316.
18. Józsi, M., M. Oppermann, J. D. Lambris, and P. F. Zipfel. 2007. The C-terminus of complement factor H is essential for host cell protection. *Mol. Immunol.* 44: 2697-2706.
19. Kajander, T., M. J. Lehtinen, S. Hyvärinen, A. Bhattacharjee, E. Leung, D. E. Isenman, S. Meri, A. Goldman, and T. S. Jokiranta. 2011. Dual interaction of factor H with C3d and glycosaminoglycans in host-nonhost discrimination by complement. *Proc. Natl. Acad. Sci. U.S.A.* 108: 2897-2902.
20. Morgan, H. P., C. Q. Schmidt, M. Guariento, B. S. Blaum, D. Gillespie, A. P. Herbert, D. Kavanagh, H. D. Mertens, D. I. Svergun, C. M. Johansson, D. Uhrín, P. N. Barlow, and J. P. Hannan. 2011. Structural basis for engagement by complement factor H of C3b on a self surface. *Nat. Struct. Mol. Biol.* 18: 463-470.
21. Aslam, M., and S. J. Perkins. 2001. Folded-back solution structure of monomeric factor H of human complement by synchrotron X-ray and neutron scattering, analytical ultracentrifugation and constrained molecular modelling. *J. Mol. Biol.* 309: 1117-1138.
22. Fakhouri, F., E. G. de Jorge, F. Brune, P. Azam, H. T. Cook, and M. C. Pickering. 2010. Treatment with human complement factor H rapidly reverses renal complement deposition in factor H-deficient mice. *Kidney Int.* 78: 279-286.
23. Sánchez-Corral, P., C. González-Rubio, S. Rodríguez de Córdoba, and M. López-Trascasa. 2004. Functional analysis in serum from atypical Hemolytic Uremic Syndrome patients reveals impaired protection of host cells associated with mutations in factor H. *Mol. Immunol.* 41: 81-84.
24. Roumenina, L. T., M. Frimat, E. C. Miller, F. Provot, M-A. Dragon-Durey, P. Bordereau, S. Bigot, C. Hue, S. C. Satchell, P. W. Mathieson, C. Mousson, C. Noel, C. Sautes-Fridman, L. Halbwachs-Mecarelli, J. P. Atkinson, A. Lionet, and V. Fremeaux-Bacchi. 2012. A prevalent C3 mutation in aHUS patients causes a direct C3 convertase gain of function. *Blood* 119: 4182-4191.
25. Józsi, M., S. Strobel, H. M. Dahse, W. S. Liu, P. F. Hoyer, M. Oppermann, C. Skerka, and P. F. Zipfel. 2007. Anti factor H autoantibodies block C-terminal recognition function of factor H in hemolytic uremic syndrome. *Blood* 110: 1516-1518.

26. Fridkis-Hareli, M., M. Storek, I. Mazsaroff, A. M. Risitano, A. S. Lundberg, C. J. Horvath, and V. M. Holers. 2011. Design and development of TT30, a novel C3d-targeted C3/C5 convertase inhibitor for treatment of human complement alternative pathway-mediated diseases. *Blood* 118: 4705-4713.
27. Kühn, S. and P. F. Zipfel. 1995. The baculovirus expression vector pBSV-8His directs secretion of histidine-tagged proteins. *Gene* 162: 225-229.
28. Castiblanco-Valencia, M. M., T. R. Fraga, L. B. Silva, D. Monaris, P. A. Abreu, S. Strobel, M. Józsi, L. Isaac, and A. S. Barbosa. 2012. Leptospiral immunoglobulin-like proteins interact with human complement regulators factor H, FHL-1, FHR-1, and C4BP. *J. Infect. Dis.* 205: 995-1004.
29. Sánchez-Corral, P., D. Pérez-Caballero, O. Huarte, A. M. Simckes, E. Goicoechea, M. López-Trascasa, and S. Rodríguez de Córdoba. 2002. Structural and functional characterization of factor H mutations associated with atypical hemolytic uremic syndrome. *Am. J. Hum. Genet.* 71: 1285-1295.
30. Thiele, G. M., L. W. Klassen, and D. J. Tuma. 2008. Formation and immunological properties of aldehyde-derived protein adducts following alcohol consumption. *Methods Mol. Biol.* 447: 235-257.
31. Ishii, T., S. Kumazawa, T. Sakurai, T. Nakayama, and K. Uchida. 2006. Mass spectroscopic characterization of protein modification by malondialdehyde. *Chem. Res. Toxicol.* 19: 122-129.
32. Koistinen, V., S. Wessberg, and J. Leikola. 1989. Common binding region of complement factors B, H and CR1 on C3b revealed by monoclonal anti-C3d. *Complement Inflamm*. 6: 270-280.
33. Jokiranta, T. S., P. F. Zipfel, J. Hakulinen, S. Kühn, M. K. Pangburn, J. D. Tamerius, and S. Meri. 1996. Analysis of the recognition mechanism of the alternative pathway of complement by monoclonal anti-factor H antibodies: evidence for multiple interactions between H and surface bound C3b. *FEBS Lett.* 393: 297-302.
34. Hebecker, M. and M. Józsi. 2012. Factor H-related protein 4 activates complement by serving as a platform for the assembly of alternative pathway C3 convertase via its interaction with C3b protein. *J. Biol. Chem.* 287: 19528-19536.
35. Strobel, S., C. Abarrategui-Garrido, E. Fariza-Requejo, H. Seeberger, P. Sánchez-Corral, and M. Józsi. 2011. Factor H-related protein 1 neutralizes anti-factor H autoantibodies in autoimmune hemolytic uremic syndrome. *Kidney Int.* 80: 397-404.
36. Strobel, S., P. F. Hoyer, C. J. Mache, E. Sulyok, W. S. Liu, H. Richter, M. Oppermann, P. F. Zipfel, and M. Józsi. 2010. Functional analyses indicate a pathogenic role of factor H autoantibodies in atypical haemolytic uraemic syndrome. *Nephrol. Dial. Transplant.* 25: 136-144.
37. Jokiranta, T. S., J. Hellwage, V. Koistinen, P. F. Zipfel, and S. Meri. 2000. Each of the three binding sites on complement factor H interacts with a distinct site on C3b. *J. Biol. Chem.* 275: 27657-27662.
38. Schmidt, C. Q., A. P. Herbert, D. Kavanagh, C. Gandy, C. J. Fenton, B. S. Blaum, M. Lyon, D. Uhrín, and P. N. Barlow. 2008. A new map of glycosaminoglycan and C3b binding sites on factor H. *J. Immunol.* 181: 2610-2619.
39. Jarva, H., T. S. Jokiranta, J. Hellwage, P. F. Zipfel, and S. Meri. 1999. Regulation of complement activation by C-reactive protein: targeting the complement inhibitory activity of factor H by an interaction with short consensus repeat domains 7 and 8-11. *J. Immunol.* 163: 3957-3962.
40. Deban, L., H. Jarva, M. J. Lehtinen, B. Bottazzi, A. Bastone, A. Doni, T. S. Jokiranta, A. Mantovani, and S. Meri. 2008. Binding of the long pentraxin PTX3 to factor H: interacting domains and function in the regulation of complement activation. *J. Immunol.* 181: 8433-8440.
41. Mihlan, M., S. Stippa, M. Józsi, and P. F. Zipfel. 2009. Monomeric CRP contributes to complement control in fluid phase and on cellular surfaces and increases phagocytosis by recruiting factor H. *Cell Death Differ.* 16: 1630-1640.
42. Okemefuna, A. I., R. Nan, A. Miller, J. Gor, and S. J. Perkins. 2010. Complement factor H binds at two independent sites to C-reactive protein in acute phase concentrations. *J. Biol. Chem.* 285: 1053-1065.
43. Kopp, A., S. Strobel, A. Tortajada, S. Rodríguez de Córdoba, P. Sánchez-Corral, Z. Prohászka, M. López-Trascasa, and M. Józsi. 2012. Atypical hemolytic uremic syndrome-associated variants and autoantibodies impair binding of factor H and factor H-related protein 1 to pentraxin 3. *J. Immunol.* 189: 1858-1867.
44. Weismann, D., K. Hartvigsen, N. Lauer, K. L. Bennett, H. P. Scholl, P. Charbel Issa, M. Cano, H. Brandstätter, S. Tsimikas, C. Skerka, G. Superti-Furga, J. T. Handa, P. F. Zipfel, J. L. Witztum, and C. J. Binder. 2011. Complement factor H binds malondialdehyde epitopes and protects from oxidative stress. *Nature* 478: 76-81.
45. Oppermann, M., T. Manuelian, M. Józsi, E. Brandt, T. S. Jokiranta, S. Heinen, S. Meri, C. Skerka, O. Götze, and P. F. Zipfel. 2006. The C-terminus of complement regulator Factor H mediates target

recognition: evidence for a compact conformation of the native protein. *Clin. Exp. Immunol.* 144: 342-352.
46. Józsi, M., C. Licht, S. Strobel, S. L. Zipfel, H. Richter, S. Heinen, P. F. Zipfel, and C. Skerka. 2008. Factor H autoantibodies in atypical hemolytic uremic syndrome correlate with CFHR1/CFHR3 deficiency. *Blood* 111: 1512-1514.
47. Blanc, C., L. T. Roumenina, Y. Ashraf, S. Hyvärinen, S. K. Sethi, B. Ranchin, P. Niaudet, C. Loirat, A. Gulati, A. Bagga, W. H. Fridman, C. Sautès-Fridman, T. S. Jokiranta, V. Frémeaux-Bacchi, and M-A. Dragon-Durey. 2012. Overall neutralization of complement factor H by autoantibodies in the acute phase of the autoimmune form of atypical hemolytic uremic syndrome. *J. Immunol.* 189: 3528-3537.
48. Noris, M., and G. Remuzzi. 2008. Translational mini-review series on complement factor H: therapies of renal diseases associated with complement factor H abnormalities: atypical haemolytic uraemic syndrome and membranoproliferative glomerulonephritis. *Clin. Exp. Immunol.* 151: 199-209.
49. Schmidt, C. Q., F. C. Slingsby, A. Richards, and P. N. Barlow. 2011. Production of biologically active complement factor H in therapeutically useful quantities. *Protein Expr. Purif.* 76: 254-263.
50. Büttner-Mainik, A., J. Parsons, H. Jérôme, A. Hartmann, S. Lamer, A. Schaaf, A. Schlosser, P. F. Zipfel, R. Reski, and E. L. Decker. 2011. Production of biologically active recombinant human factor H in Physcomitrella. *Plant Biotechnol. J.* 9: 373-383.
51. Perkins, S. J., R. Nan, K. Li, S. Khan, and A. Miller. 2012. Complement factor H-ligand interactions: self-association, multivalency and dissociation constants. *Immunobiology* 217: 281-297.
52. Laine, M., H. Jarva, S. Seitsonen, K. Haapasalo, M. J. Lehtinen, N. Lindeman, D. H. Anderson, P. T. Johnson, I. Järvelä, T. S. Jokiranta, G. S. Hageman, I. Immonen, and S. Meri. 2007. Y402H polymorphism of complement factor H affects binding affinity to C-reactive protein. *J. Immunol.* 178: 3831-3836.
53. Skerka, C., N. Lauer, A. A. Weinberger, C. N. Keilhauer, J. Sühnel, R. Smith, U. Schlötzer-Schrehardt, L. Fritsche, S. Heinen, A. Hartmann, B. H. Weber, and P. F. Zipfel. 2007. Defective complement control of factor H (Y402H) and FHL-1 in age-related macular degeneration. *Mol. Immunol.* 44: 3398-3406.
54. Lauer, N., M. Mihlan, A. Hartmann, U. Schlötzer-Schrehardt, C. Keilhauer, H. P. Scholl, P. Charbel Issa, F. Holz, B. H. Weber, C. Skerka, and P. F. Zipfel. 2011. Complement regulation at necrotic cell lesions is impaired by the age-related macular degeneration-associated factor-H His402 risk variant. *J. Immunol.* 187: 4374-4383.
55. Clark, S. J., L. A. Ridge, A. P. Herbert, S. Hakobyan, B. Mulloy, R. Lennon, R. Würzner, B. P. Morgan, D. Uhrín, P. N. Bishop, and A. J. Day. 2013. Tissue-specific host recognition by complement factor H is mediated by differential activities of its glycosaminoglycan-binding regions. *J. Immunol.* 190: 2049-2057.
56. Jokiranta, T. S., A. Solomon, M. K. Pangburn, P. F. Zipfel, and S. Meri. 1999. Nephritogenic lambda light chain dimer: a unique human miniautoantibody against complement factor H. *J. Immunol.* 163: 4590-4596.
57. Nozal, P., S. Strobel, M. Ibernon, D. López, P. Sánchez-Corral, S. Rodríguez de Córdoba, M. Józsi, and M. López-Trascasa. 2012. Anti-factor H antibody affecting factor H cofactor activity in a patient with dense deposit disease. *Clin. Kidney J.* 5: 133-136.
58. Goodship, T. H., I. Y. Pappworth, T. Toth, M. Denton, K. Houlberg, F. McCormick, D. Warland, I. Moore, E. M. Hunze, S. J. Staniforth, C. Hayes, D. P. Cavalcante, D. Kavanagh, L. Strain, A. P. Herbert, C. Q. Schmidt, P. N. Barlow, C. L. Harris, and K. J. Marchbank. 2012. Factor H autoantibodies in membranoproliferative glomerulonephritis. *Mol. Immunol.* 52: 200-206.
59. Meri, S. 2007. Loss of self-control in the complement system and innate autoreactivity. *Ann. N. Y. Acad. Sci*. 1109: 93-105.
60. Zipfel, P. F., and N. Lauer. 2013. Defective complement action and control defines disease pathology for retinal and renal disorders and provides a basis for new therapeutic approaches. *Adv. Exp. Med. Biol.* 735: 173-187.
61. Goicoechea de Jorge, E., C. L. Harris, J. Esparza-Gordillo, L. Carreras, E. A. Arranz, C. A. Garrido, M. López-Trascasa, P. Sánchez-Corral, B. P. Morgan, and S. Rodríguez de Córdoba. 2007. Gain-of-function mutations in complement factor B are associated with atypical hemolytic uremic syndrome. *Proc. Natl. Acad. Sci. U S A.* 104: 240-245.
62. Roumenina, L. T., M. Jablonski, C. Hue, J. Blouin, J. D. Dimitrov, M.A. Dragon-Durey, M. Cayla, W. H. Fridman, M. A. Macher, D. Ribes, L. Moulonguet, L. Rostaing, S. C. Satchell, P. W. Mathieso,

C. Sautes-Fridman, C. Loirat, C. H. Regnier, L. Halbwachs-Mecarelli, and V. Fremeaux-Bacchi. 2009. Hyperfunctional C3 convertase leads to complement deposition on endothelial cells and contributes to atypical hemolytic uremic syndrome. *Blood* 114: 2837-2845.
63. Martínez-Barricarte, R., M. Heurich, F. Valdes-Cañedo, E. Vazquez-Martul, E. Torreira, T. Montes, A. Tortajada, S. Pinto, M. Lopez-Trascasa, B. P. Morgan, O. Llorca, C. L. Harris, and Rodríguez de Córdoba S. 2010. Human C3 mutation reveals a mechanism of dense deposit disease pathogenesis and provides insights into complement activation and regulation. *J. Clin. Invest.* 120: 3702-3712.
64. Sartz, L., A. I. Olin, A. C. Kristoffersson, A. L. Ståhl, M. E. Johansson, K. Westman, V. Fremeaux-Bacchi, K. Nilsson-Ekdahl, and D. Karpman. 2012. A novel C3 mutation causing increased formation of the C3 convertase in familial atypical hemolytic uremic syndrome. *J. Immunol.* 188: 2030-2037.
65. Paixão-Cavalcante, D., M. López-Trascasa, L. Skattum, P. C. Giclas, T. H. Goodship, S. Rodríguez de Córdoba, L. Truedsson, B. P. Morgan, and C. L. Harris. 2012. Sensitive and specific assays for C3 nephritic factors clarify mechanisms underlying complement dysregulation. *Kidney Int.* 82: 1084-1092.
66. Risitano, A. M. 2012. Paroxysmal nocturnal hemoglobinuria and other complement-mediated hematological disorders. *Immunobiology* 217: 1080-1087.
67. Ferreira, V. P. and M. K. Pangburn. 2007. Factor H mediated cell surface protection from complement is critical for the survival of PNH erythrocytes. *Blood* 110: 2190-2192.
68. Risitano, A. M., R. Notaro, C. Pascariello, M. Sica, L. del Vecchio, C. J. Horvath, M. Fridkis-Hareli, C. Selleri, M. A. Lindorfer, R. P. Taylor, L. Luzzatto, and V. M. Holers. 2012. The complement receptor 2/factor H fusion protein TT30 protects paroxysmal nocturnal hemoglobinuria erythrocytes from complement-mediated hemolysis and C3 fragment. *Blood* 119: 6307-6316.

Footnotes

[1]This work was presented in part at the 24th International Complement Workshop, Chania, Greece in October 2012 (Immunobiology, 217:1137).
This work was financially supported by the Deutsche Forschungsgemeinschaft (grant JO 844/1-1 to M.J.), the Hungarian Academy of Sciences (LP2012-43/2012 to M.J.), by the Spanish Instituto de Salud Carlos III (grant PS09/00268 to P.S-C.), by the Academy of Finland (projects 128646 and 259793) and Sigrid Juselius Foundation (grant to T.S.J), and by Agence Nationale de la Recherche, France (ANR Genopath 2009-2012 09geno03101I) and by INSERM. M.A-D. is supported by the Spanish Comunidad de Madrid (grant S2010/BMD-2316).

[2]Corresponding author: Mihály Józsi, MTA-ELTE "Lendület" Complement Research Group, Department of Immunology, Eötvös Loránd University, Pázmány Péter sétány 1/c, H-1117 Budapest, Hungary; Phone: +36 1 3812175; Fax: +36 1 3812176; E-mail: mihaly.jozsi@gmx.net.

[3]Abbreviations used in this paper: aHUS, atypical hemolytic uremic syndrome; AMD, age-related macular degeneration; CCP, complement control protein domain; CFHR1, factor H-related protein 1; CRP, C-reactive protein; DDD, dense deposit disease; DPBS, Dulbecco's phosphate-buffered saline; ECM, extracellular matrix; FH, factor H; HSA, human serum albumin; MDA, malondialdehyde; MAA-BSA, malondialdehyde-acetaldehyde-adduct of BSA; PNH, paroxysmal nocturnal hemoglobinuria; PTX3, pentraxin 3.

Author contributions

M.J. initiated the study. M.H., P.S-C., L.T.R. and M.J. designed the experiments. M.H. performed protein expression, cofactor and decay acceleration assays. S.R. performed cloning and protein expression. M.A-D., P.S-C., M-A.D-D. and M.J. performed hemolysis assays. L.T.R., S.H., T.S.J. and M.J. performed ligand binding assays. L.T.R. and M.J. performed the endothelial cell assays. P.S-C. and M.J. wrote the manuscript with the help of other authors.

Figure legends

Figure 1. Generation and characterization of mini-FH.

(A) Schematic representation of mini-FH. FH is composed of 20 domains. Domains 1-4 mediate the complement regulatory activities of FH, and domains 19-20 mediate its attachment to host cells and basement membranes. To generate mini-FH, these two major functional regions were directly fused together. (B) Schematic drawing of FH engaging C3b on a host surface, based on structural data (15, 19, 20) (left panel),

and hypothesized action of mini-FH (right panel). (C) Silver staining of purified mini-FH. 1.2 µg mini-FH was run on 11% SDS-PAGE and stained with silver nitrate. The molecular weight marker is shown on the left (kDa).

Figure 2. Interaction of mini-FH with C3 fragments measured by ELISA.
ELISA assays to analyze the interaction of mini-FH/FH with C3b and C3d. Mini-FH and FH were immobilized in microtiter plates at 100 nM. Serial dilutions of fluid-phase C3b (A) or C3d (B) were added and their binding detected using anti-C3 and anti-C3d antibodies, respectively. Data are mean ± SD from three experiments. The binding of C3d to mini-FH was significantly stronger than to FH ($p < 0.001$, two-way ANOVA).

Figure 3. Comparison of the interaction of mini-FH and factor H with C3b and C3d by surface plasmon resonance assay.
(A) C3b and (B) C3d were immobilized on a sensor chip and the binding of FH (left panels) and mini-FH (right panels) injected in the fluid phase at 50 nM, 25 nM, 12.5 nM, 6.25 nM and 3.12 nM concentration was measured in real time. The black lines represent the obtained experimental sensorograms and the gray lines are the fitted curves. The chi^2 values for the fitted curves were 37.4 for FH–C3b, 6.35 for FH–C3d, 66.6 for mini-FH–C3b, and 92.1 for mini-FH–C3d. A representative experiment out of three performed is shown.

Figure 4. Decay accelerating and cofactor activity of mini-FH.
(A) Decay acceleration assay. The alternative pathway C3 convertase (C3bBb) was assembled on microtiter plates. FH, mini-FH, or human serum albumin (HSA) as a control, were added and the remaining intact convertase was detected after 30 min using anti-factor B antibody. Data are mean ± SD from three experiments. The convertase decay accelerating effects of mini-FH and FH were statistically not significantly different from each other (two-way ANOVA). (B) The cofactor activity of mini-FH in the fluid phase was measured by incubating C3b with factor I and 10 nM FH or mini-FH at 37°C for 1 h. C3b proteolysis was visualized after performing 11% SDS-PAGE and Western blotting using polyclonal anti-C3 antibody. The C3b cleavage products are indicated on the right. The blot is representative of three experiments.

Figure 5. Mini-FH is functionally active when bound to pentraxins.
(A) Pentraxin 3 (PTX3) and C-reactive protein (CRP) were immobilized in microtiter plate wells. Binding of mini-FH and FH was detected using a FH antiserum. Data represent mean ± SD from three experiments. FH bound more strongly to CRP than mini-FH ($p<0.001$, two-way ANOVA) whereas the binding of FH and mini-FH to PTX3 was similar. (B) The cofactor activity of PTX3- and CRP-bound mini-FH and FH, added at 1 µM, was measured after incubation with C3b and factor I. Supernatants were analyzed by 11% reducing SDS-PAGE followed by Western blotting using an anti-C3 antibody to detect C3b degradation fragments. A representative blot out of two experiments is shown.

Figure 6. Mini-FH binds to MDA-epitopes.
(A) Binding of FH, mini-FH and FH1-4 (0.13 µM) to MAA-BSA immobilized in microtiter plate wells. The binding was detected with the mAb 90X. Data represent mean ± SD of five values. The binding of FH to MAA-BSA was significantly stronger than that of mini-FH ($p<0.001$, one-way ANOVA). (B) Dose-dependent binding of mini-FH to MAA-BSA. As control, FH1-4 was used. Binding was measured as in (A).

Figure 7. Mini-FH binds to the extracellular matrix.
(A) Microtiter plates were coated with the human basement membrane extract MaxGel or gelatin as control. Binding of mini-FH and FH was detected using a FH antiserum. Data represent mean ± SD from three experiments. The binding of mini-FH and FH to MaxGel was not significantly different from each other (two-way ANOVA). (B) The cofactor activity of MaxGel-bound mini-FH and FH, added at 1 µM, was measured as described in Fig. 5B. A representative blot out of two experiments is shown.

Figure 8. Mini-FH is functionally active when bound to endothelial cells.
(A) Binding of 2 µM mini-FH or FH to HUVEC was analyzed by flow cytometry as described in Materials and methods. Representative histograms out of three experiments are shown. (B) Binding of mini-FH and FH was also visualized from HUVEC extracts, which were separated on 11% SDS-PAGE and subjected to Western blotting using a FH antiserum. (C) The cofactor activity of HUVEC-bound mini-FH or FH, added at

2 μM, was measured after adding C3b and factor I. C3b cleavage was analyzed in the supernatants by Western blotting as described in the legend to Fig. 5. In (B) and (C), representative blots out of two experiments are shown. (D) HUVEC were activated with TNFα, IFNγ and IL-1 as described in Materials and methods, and incubated for 30 min with 30% FH-depleted serum in the presence of 5 mM Ca^{2+} and Mg^{2+} and the indicated concentrations of FH or mini-FH. C3 deposition on the cells was determined by flow cytometry using an anti-C3c antibody. Data represent means ± SD from three experiments. The difference between the inhibitory activity of FH and mini-FH was statistically significant (p=0.0009, two-way ANOVA).

Figure 9. Mini-FH reverses the anomalous hemolysis caused by aHUS-associated FH mutations or autoantibodies.
(A) Mini-FH binds to SRBC. SRBC were incubated with 15% C2-depleted human serum (C2depl), with or without 2 μM mini-FH and FH-related protein 1 (CFHR1). SRBC were washed and lysed, and the lysates subjected to 12% SDS-PAGE and Western blotting using a FH antiserum. A representative blot out of three is shown. (B) Mini-FH does not induce SRBC hemolysis in human serum. SRBC were incubated as described in (A) with 2 μM mini-FH, CFHR1 or the FH fragment consisting CCPs 15-20 (FH15-20). After 30 min, hemoglobin in the supernatants was measured. In a control sample, water was added to achieve total SRBC lysis (white bar). Compared to the negative control (C2-depleted serum only), CFHR1 and mini-FH did not increase SRBC lysis, whereas FH15-20 significantly increased cell lysis (p<0.01, one-way ANOVA). (C) SRBC lysis was induced in 15% C2-depleted serum by the mAb C18, which blocks FH binding to the cells. Mini-FH and FH were added in the indicated concentrations, and the extent of hemolysis was determined as described in (B). The difference between the inhibitory activity of FH and mini-FH was statistically significant (p<0.001, two-way ANOVA). (D) SRBC were lysed by 10% serum from an aHUS patient with anti-FH autoantibodies or (E) from an aHUS patient carrying the W1183L mutation in CCP20 in heterozygosis. (F) SRBC lysis was induced in 10% human serum by the mAb OX24, which blocks the complement regulatory activity of FH. The effect of mini-FH and FH on the hemolysis was determined as described in (B). The difference between the inhibitory activity of FH and mini-FH was statistically significant (p=0.0063, two-way ANOVA). In (B), (C) and (F), data represent mean ± SD from three experiments. In (D) and (E), representative data from two experiments are shown.

Figure 10. Mini-FH reverses the anomalous hemolysis caused by autoantibodies directed against multiple FH epitopes.
Plasma samples from three patients diagnosed with autoimmune aHUS were collected at the very onset. The autoantibodies in these samples bound to the N- and C-terminal parts of FH, in patient 2 also to the central part (domains 8-11). Non-sensitized SRBC were incubated with the patients' plasma diluted 6, 10 and 15%, respectively. Increasing amounts of mini-FH or FH were added before performing the assay as described (47). Data are representative of two experiments.

Table I. Kinetic parameters of the interaction of factor H and mini-factor H with C3b and C3d.

C3b	$k_a \times 10^4$ (1/Ms)	$k_d \times 10^{-2}$ (1/s)	$K_D \times 10^{-7}$ (M)	RU at 400 s at 25 nM
Factor H	9.58 ± 0.76	4.21 ± 0.85	4.41 ± 0.9	38.66 ± 2.89
Mini-factor H	3.62 ± 0.11	3.21 ± 0.53	8.88 ± 1.45	122.37 ± 23
t-test (n = 3)	p = 0.006	p = 0.76	p = 0.05	p = 0.003
C3d	$k_a \times 10^4$ (1/Ms)	$k_d \times 10^{-2}$ (1/s)	$K_D \times 10^{-6}$ (M)	RU at 400 s at 25 nM
Factor H	5.01 ± 0.31	32.4 ± 4.81	6.45 ± 0.57	5.35 ± 1.95
Mini-factor H	0.59 ± 0.3	1.45 ± 0.03	2.46 ± 0.06	452.06 ± 75
t-test (n = 3)	p = 0.004	p = 0.004	p = 0.01	p = 0.001

Association and dissociation rates were determined by surface plasmon resonance analysis. The apparent dissociation rate constants (K_D) were calculated from the rate constants. RU, resonance unit

Figure 1 (Józsi)

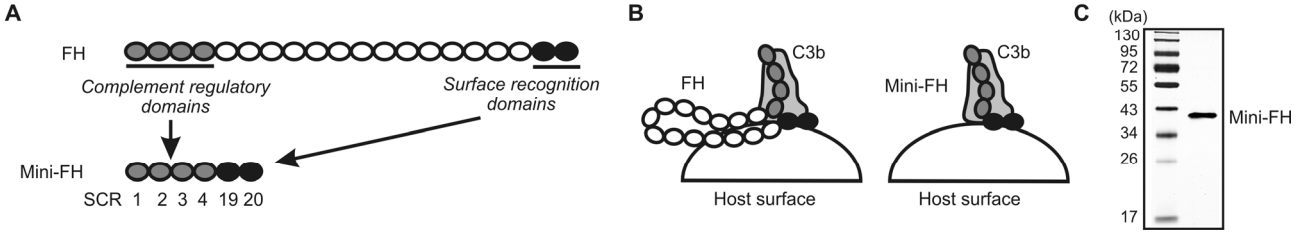

Figure 2 (Józsi)

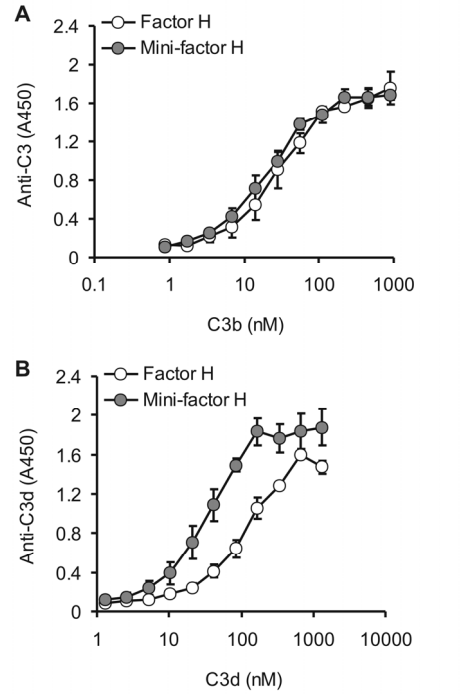

Figure 3 (Józsi)

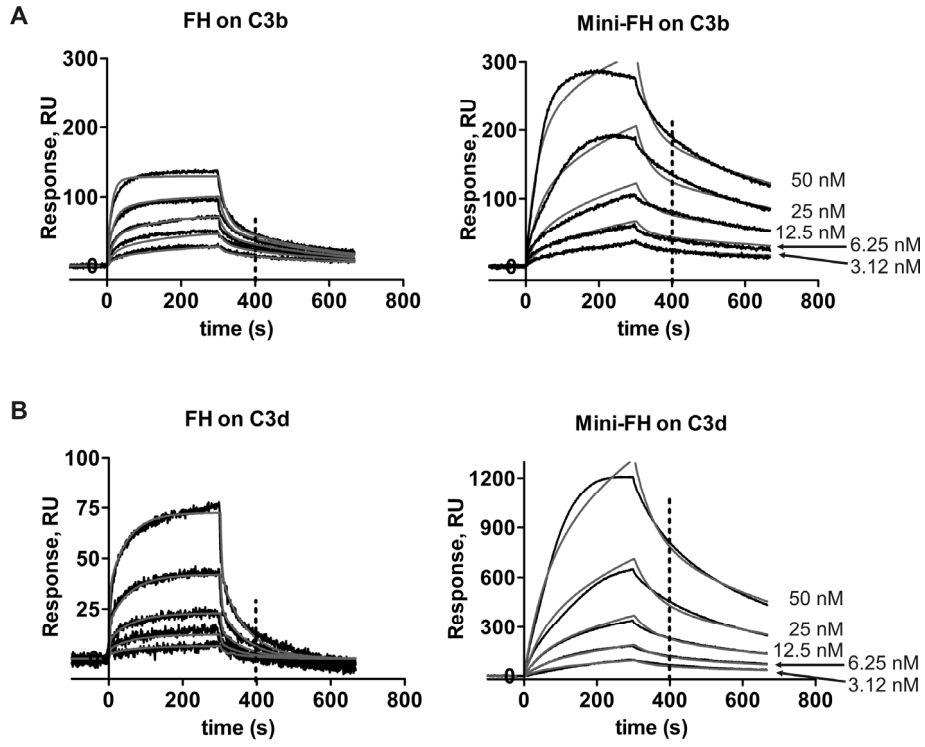

Figure 4 (Józsi)

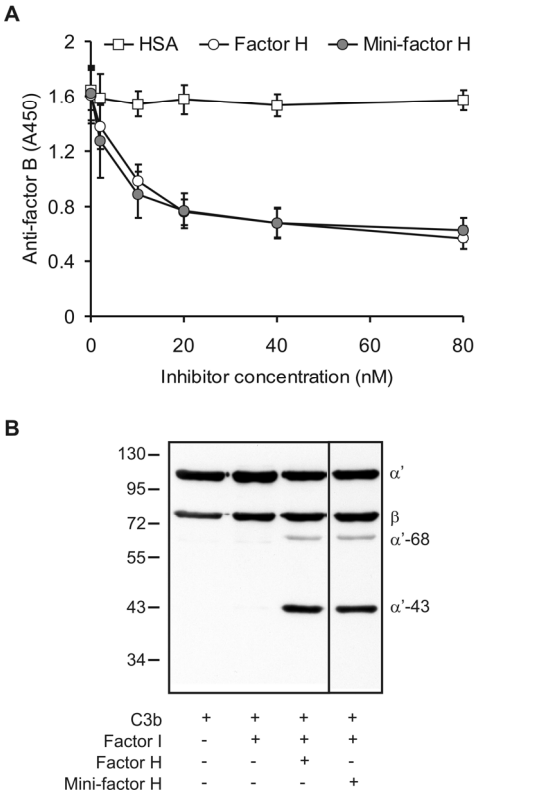

Figure 5 (Józsi)

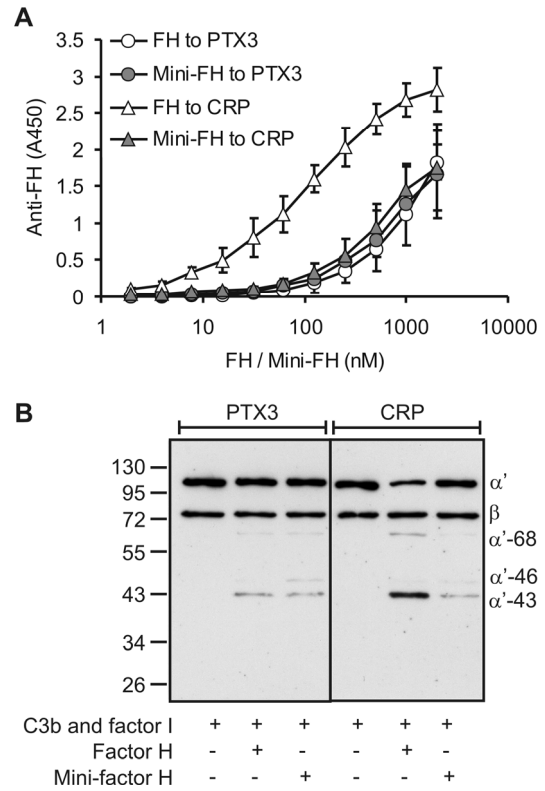

Figure 6 (Józsi)

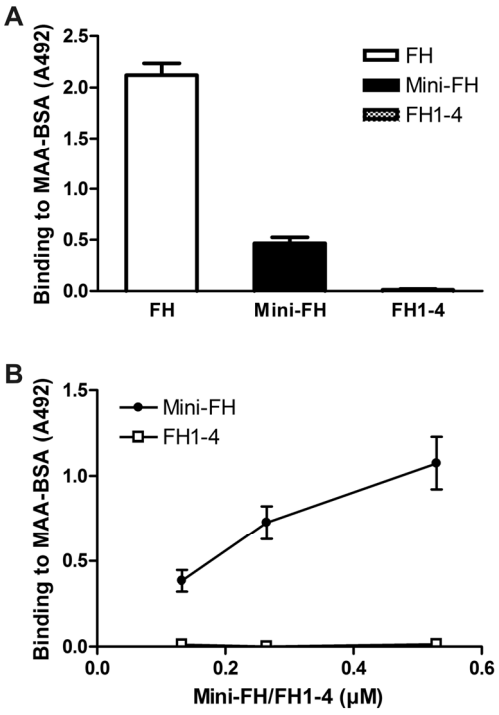

Figure 7 (Józsi)

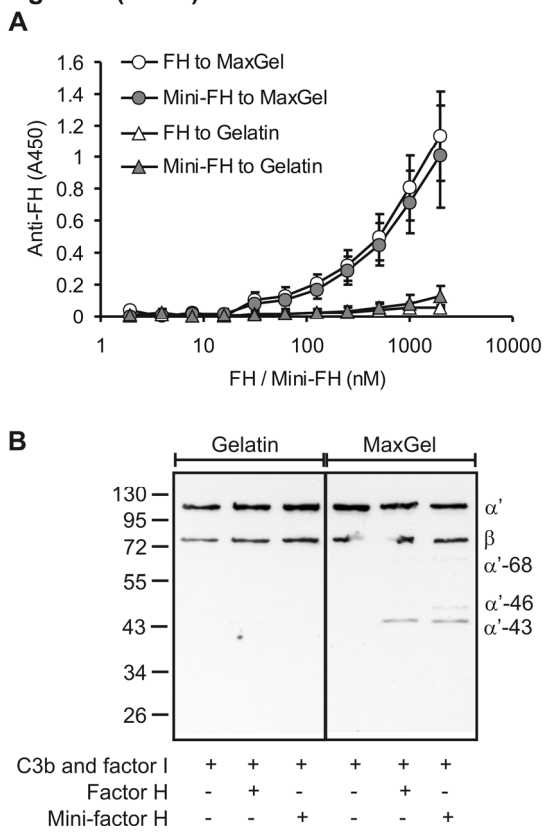

Figure 8 (Józsi)

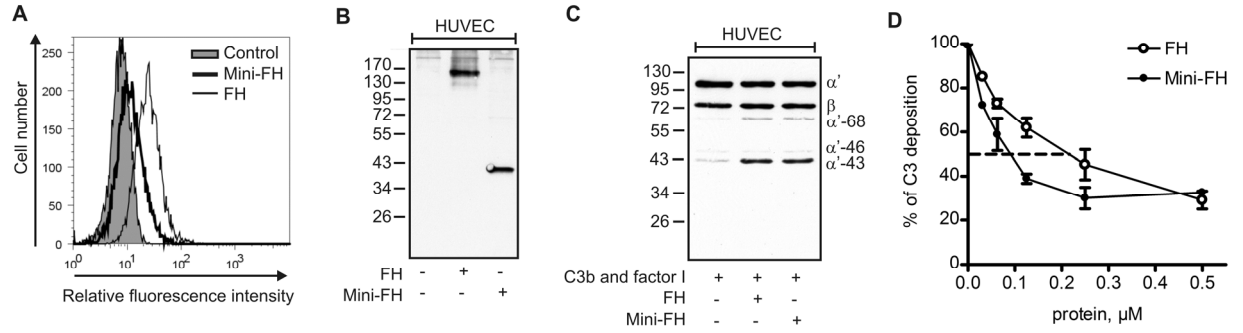

Figure 9 (Józsi)

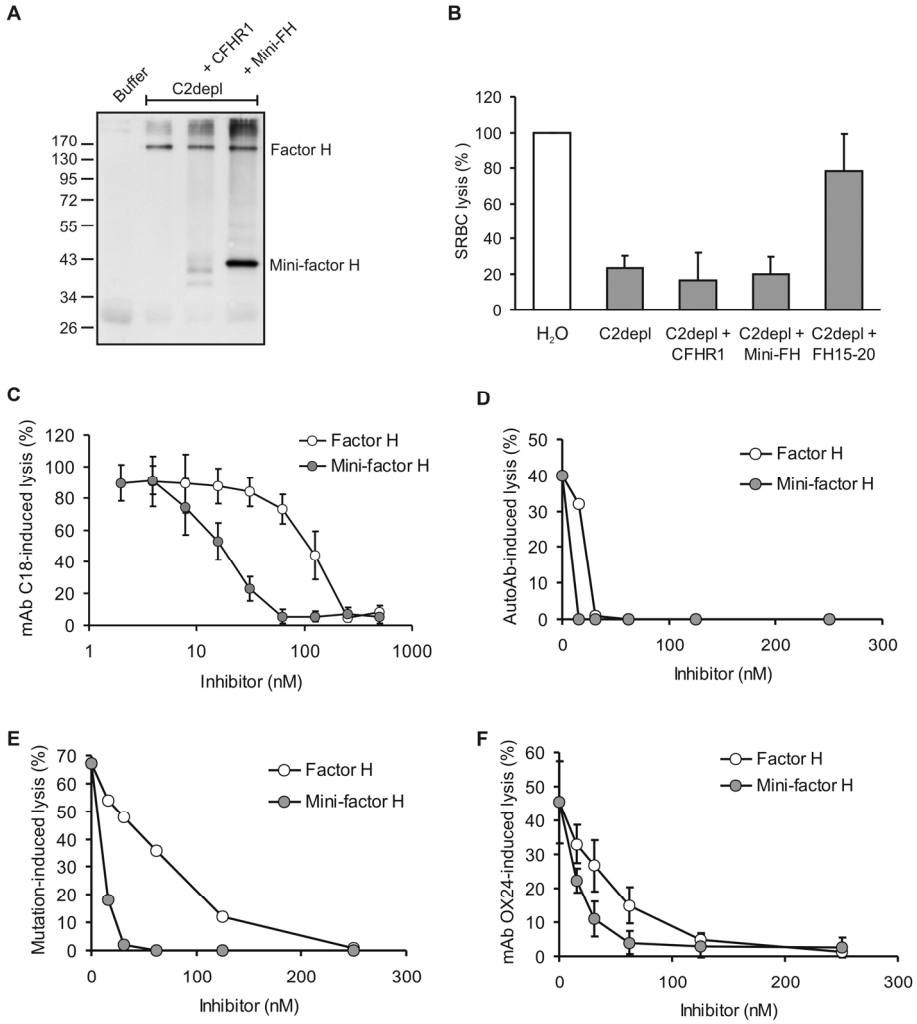

Figure 10 (Józsi)

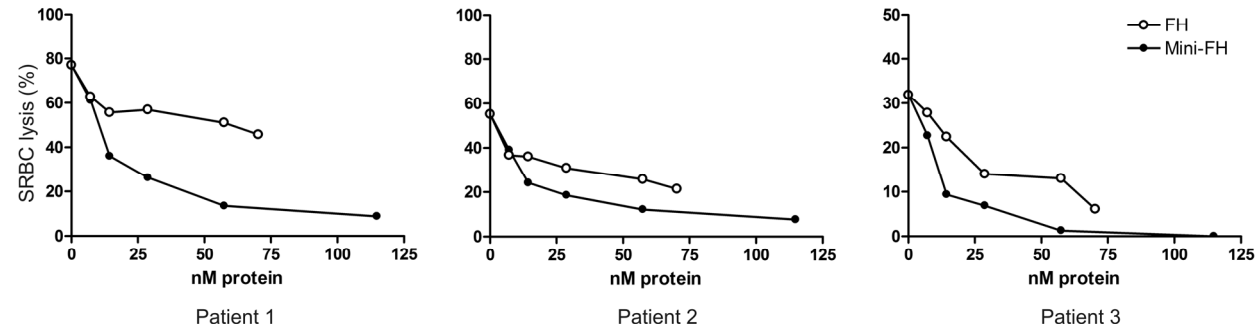

Supplemental Figure 1

```
gaagactgtaacgaactgcccccgagacgcaacaccgaaatcctgaccggctcatggagc
 E  D  C  N  E  L  P  P  R  R  N  T  E  I  L  T  G  S  W  S  20
gaccaaacatacccagagggaacccaggctatctacaagtgcaggccaggttacagaagc
 D  Q  T  Y  P  E  G  T  Q  A  I  Y  K  C  R  P  G  Y  R  S  40
ctcggcaacgttatcatggtgtgtcgcaagggagagtgggtggccttgaaccccctgagg
 L  G  N  V  I  M  V  C  R  K  G  E  W  V  A  L  N  P  L  R  60
aagtgccagaagagaccctgtggacaccctggtgacaccccattcggtaccttcactttg
 K  C  Q  K  R  P  C  G  H  P  G  D  T  P  F  G  T  F  T  L  80
acaggtggcaacgtcttcgagtacggcgtcaaggctgtttacacttgcaacgaaggatac
 T  G  G  N  V  F  E  Y  G  V  K  A  V  Y  T  C  N  E  G  Y  100
caactgctcggcgagatcaactacagggaatgcgacaccgatggctggactaacgacatc
 Q  L  L  G  E  I  N  Y  R  E  C  D  T  D  G  W  T  N  D  I  120
cctatctgcgaggtggtcaagtgtctgccggtgactgctcccgaaaacggaaagatcgtc
 P  I  C  E  V  V  K  C  L  P  V  T  A  P  E  N  G  K  I  V  140
tcctctgccatggagccagaccgtgaataccacttcggtcaggccgtgcgcttcgtctgc
 S  S  A  M  E  P  D  R  E  Y  H  F  G  Q  A  V  R  F  V  C  160
aactccggctacaagatcgagggagatgaggaaatgcactgttctgacgatggcttctgg
 N  S  G  Y  K  I  E  G  D  E  E  M  H  C  S  D  D  G  F  W  180
agcaaggagaagcctaagtgcgttgaaatctcttgtaagagcccggacgtcatcaacgga
 S  K  E  K  P  K  C  V  E  I  S  C  K  S  P  D  V  I  N  G  200
tcacctatctcgcagaagatcatctacaaggagaacgaacgtttccaatacaagtgcaac
 S  P  I  S  Q  K  I  I  Y  K  E  N  E  R  F  Q  Y  K  C  N  220
atgggttacgagtactcagaacgtggcgacgctgtgtgtactgagtcgggttggcgccca
 M  G  Y  E  Y  S  E  R  G  D  A  V  C  T  E  S  G  W  R  P  240
ttgccgtcctgcgaagattctaccggcaagtgtggacccccctccaccgatcgacaacggc
 L  P  S  C  E ‖D  S  T  G  K  C  G  P  P  P  P  I  D  N  G  260
gatatcacaagcttccctctgtcagtctacgctccagccagctcagttgagtaccagtgc
 D  I  T  S  F  P  L  S  V  Y  A  P  A  S  S  V  E  Y  Q  C  280
caaaacctctaccagttggaaggaaacaagcgtatcacctgccgcaacggtcaatggtcc
 Q  N  L  Y  Q  L  E  G  N  K  R  I  T  C  R  N  G  Q  W  S  300
gagccccctaagtgcctgcacccctgtgtcatctctagggagatcatggaaaactacaac
 E  P  P  K  C  L  H  P  C  V  I  S  R  E  I  M  E  N  Y  N  320
atcgctctgaggtggacagccaagcagaagctctactcgagaaccggcgagtccgttgaa
 I  A  L  R  W  T  A  K  Q  K  L  Y  S  R  T  G  E  S  V  E  340
ttcgtgtgcaagcgtggataccgcctctcgtccagatcccacaccctgagaactacctgc
 F  V  C  K  R  G  Y  R  L  S  S  R  S  H  T  L  R  T  T  C  360
tgggacggaaagctggaatacccgacttgcgctaagagg
 W  D  G  K  L  E  Y  P  T  C  A  K  R                       373
```

Figure S1. Nucleotide and amino acid sequence of codon-optimized mini-FH.
The 1119 nucleotide long sequence of FH exons coding for domains 1-4 and domains 19-20 were codon-optimized for expression in insect cells. The translated protein sequence is shown below the nucleotide sequence. The linker between CCP4 and CCP19 is shown in bold, the boundary is indicated by a double vertical line.